Qiu *et al. Natural Products and Bioprospecting* (2026) 16:57
https://doi.org/10.1007/s13659-026-00629-9

Natural Products and Bioprospecting

ORIGINAL ARTICLE Open Access

Prenylated acylphloroglucinols from the fruits of *Hypericum patulum*

Yu-Feng Qiu[1†], Yi Zhou[1†], Cheng Chen[3], Juan Huang[2*] and Xing-Wei Yang[1*]

Abstract

Twenty-eight prenylated acylphloroglucinols, including the new hypulatones C–F (**1**–**4**), have been isolated from the fruits of *Hypericum patulum* and structurally characterized. Compound **1** represents a rare meroterpenoid formed through the addition of a prenylated acylphloroglucinol unit and a sesquiterpenoid moiety. Spirocyclic polycyclic polyprenylated acylphloroglucinol **2** contains six chiral centers, and its relative configuration was established based on ^{1}H–^{1}H coupling constants, conformational analysis, and NOE correlations. The cytotoxic activities of all isolates against two human carcinoma cell lines (Huh-7 and Panc-1) were evaluated using the CCK-8 assay. Bioassay results indicated that compounds **6**, **8**, and **15** exhibited moderate antiproliferative activity.

Keywords Prenylated acylphloroglucinols, *Hypericum patulum*, Structural determination, Cytotoxicity

†Yu-Feng Qiu and Yi Zhou have contributed equally to this work.

*Correspondence:
Juan Huang
huang_juan_2020@163.com
Xing-Wei Yang
yang-xingwei@foxmail.com
Full list of author information is available at the end of the article

Graphical Abstract

Hypericum patulum

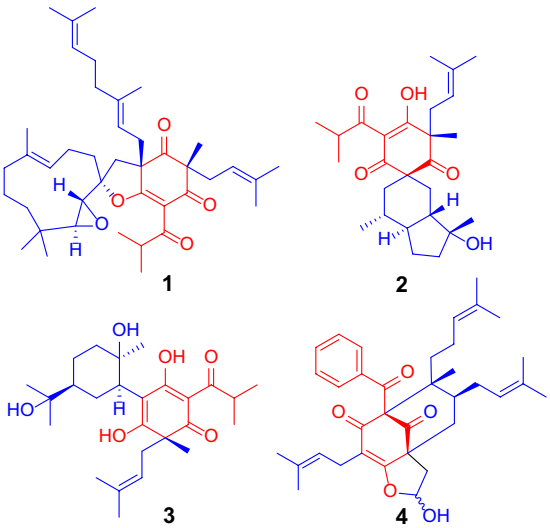

1 Introduction

Polyprenylated acylphloroglucinols (PAPs) are a class of structurally fascinating hybrid natural products that exhibit diverse bioactivities, such as tumor inhibitive, antimicrobial, HIV preventative, antioxidant, and antidepressant [1, 2]. Plants of the genus *Hypericum* (Hypericaceae) are known to be a rich source of PAPs. *Hypericum patulum*, commonly known as "Jinsimei", is a *Hypericum* species primarily distributed in southwestern China, notably in Yunnan, Guizhou, and Sichuan provinces [3]. It is a traditional Chinese medicine commonly used for the treatment of hepatitis, bacterial diseases, and epistaxis [4]. Due to the structural diversity of its chemical constituents and their potential pharmacological effects, this plant has attracted widespread scientific interest [5–17]. As we have a longstanding interest in the investigation of structures and bioactivities of PAPs [1, 18–30], we selected the fruit of *H. patulum* for further investigation. Four undescribed PAPs, hypulatones C–F (**1**–**4**), were isolated together with twenty-four known analogues (**5**–**28**, Figs. 1 and 2). Compound **1** represents a rare meroterpenoid formed through the addition of a prenylated acylphloroglucinol unit and a sesquiterpenoid moiety. To date, only eight enantiomeric pairs of this type of meroterpenoids have been reported [14, 31]. Herein are described the isolation, structure determination, and inhibitory activities against two human carcinoma cells (Huh-7 and Panc-1) of all the compounds isolated. This study provides an effective method for configurational assignments of spirocyclic polycyclic polyprenylated acylphloroglucinols (PPAPs) that bear six chiral centers.

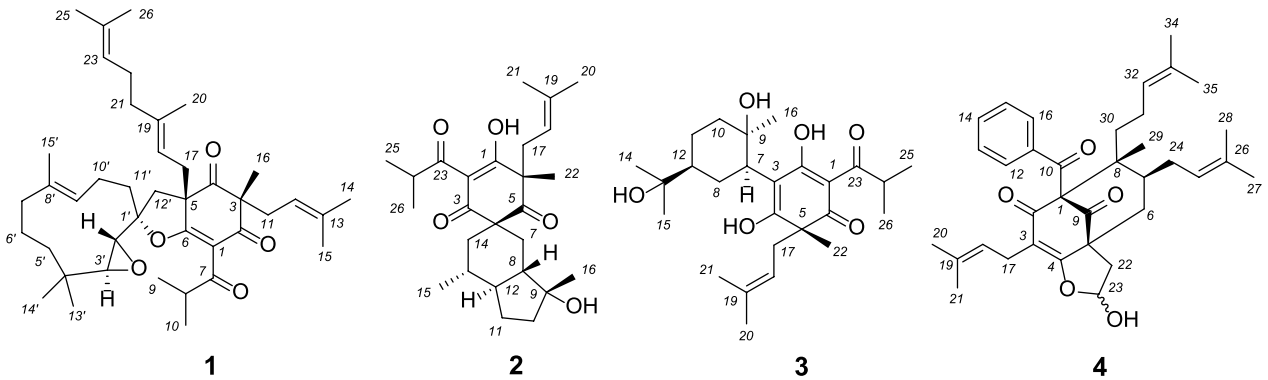

Fig. 1 The structures of compounds **1**–**4**

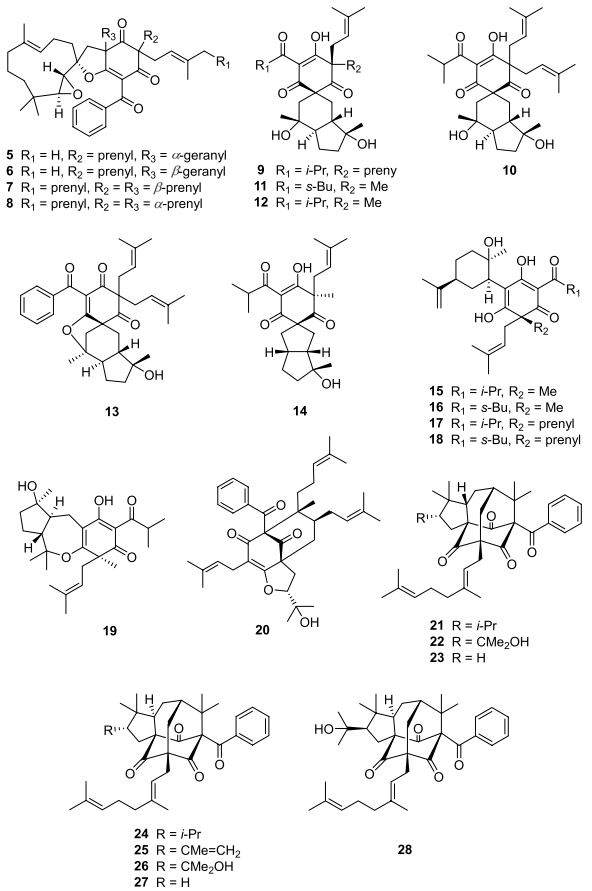

Fig. 2 The structures of compounds **5**–**28**

Table 1 ^{13}C (150 MHz) and ^{1}H NMR (600 MHz) data of compound **1** in $CDCl_3$

No	δ_C, type	δ_H mult. (*J* in Hz)	No	δ_C, type	δ_H mult. (*J* in Hz)
1	115.3, C		23	123.9, CH	5.02, t (6.3)
2	199.3, C		24	131.5, C	
3	57.4, C		25	25.7, CH_3	1.67, s
4	207.4, C		26	17.7, CH_3	1.59, s
5	62.6, C		1′	92.4, C	
6	178.7, C		2′	59.4, CH	2.63, d (2.0)
7	203.2, C		3′	64.2, CH	2.85, d (2.0)
8	39.8, CH	3.07, sept (6.9)	4′	33.8, C	
9	18.5, CH_3	1.09, d (6.9)	5′	39.3, CH_2	1.57, overlap
10	18.1, CH_3	1.16, d (6.9)			1.24, m
11	39.5, CH_2	2.67, dd (13.8, 7.8)	6′	20.2, CH_2	1.57, overlap
		2.31, dd (13.8, 7.8)			1.41, m
12	118.6, CH	4.82, t (7.8)	7′	39.5, CH_2	2.02, overlap
13	135.3, C				1.76, t (12.6)
14	26.0, CH_3	1.58, s	8′	135.5, C	
15	17.4, CH_3	1.53, s	9′	123.6, CH	5.13, dd (10.2, 4.0)
16	21.8, CH_3	1.31, s	10′	23.3, CH_2	2.41, m
17	40.3, CH_2	3.29, dd (15.0, 9.3)			1.95, overlap
		2.28, dd (15.0, 4.0)	11′	40.3, CH_2	1.97, overlap
18	116.6, CH	4.74, dd (9.3, 4.0)			1.71, m
19	141.4, C		12′	41.0, CH_2	2.31, s
20	17.6, CH_3	1.62, s	13′	25.3, CH_3	1.00, s
21	39.9, CH_2	1.97, m	14′	22.4, CH_3	0.64, s
22	26.3, CH_2	2.03, m	15′	16.3, CH_3	1.64, s

2 Results and discussion

Hypulatone C (**1**) was obtained as yellow gum. Its molecular formula $C_{41}H_{60}O_5$ with 12 degrees of unsaturation was established by analysis of ^{13}C NMR (Table 1) and HRESIMS data (*m/z* 671.4082, $[M+K]^+$, cacld for 671.4072). The FTIR spectrum displayed absorption bands due to carbonyl (1719 and 1699 cm^{-1}) functionalities. The ^{1}H NMR spectrum (Table 1) exhibited the signals of an isopropyl (δ_H 3.07, sept; 1.16, d; 1.09, d; $J=6.9$ Hz), four olefinic protons (δ_H 4.51–5.01), and nine singlet methyls (δ_H 0.64–1.67). Analysis of its ^{13}C and DEPT-NMR data revealed a total of 41 carbon resonances, including a shielded sp^2 carbon at δ_C 115.3 (C-1) and three deshielded carbons at δ_C 178.7 (C-6), 199.3 (C-2), and 203.2 (C-7), which were indicative of the presence of an enol-β-triketo system. The above signals, in combination with a nonconjugated ketone at δ_C 207.4 (C-4) and two quaternary carbons at δ_C 57.4 (C-3) and 62.6 (C-5), suggested that compound **1** should possess a dearomatized acylphloroglucinol core. This assumption was further confirmed by the HMBC correlations from a singlet methyl at δ_H 1.31 (Me-16) to C-2, C-3, and C-4, and from δ_H 3.29 and 2.28 (H_2-17) to C-4, and C-5, and C-6. An isoprenyl group (δ_C 39.5, C-11; 118.6, C-12; 135.3, C-13; 26.0, C-14; 17.4, C-15) linked to C-3 was deduced by the correlation of δ_H 4.82 (H-12)/δ_H 2.67 and 2.31 (H_2-11) in the ^{1}H–^{1}H COSY spectrum, together with the correlations of both δ_H 1.58 (Me-14) and 1.53 (Me-15) with C-11 and C-12, of H_2-11 with C-2, C-3, and C-4 in the HMBC spectrum. Moreover, C-17 was proved to be the head of a geranyl group (δ_C 40.3, C-17; 116.6, C-18; 141.4, C-19; 17.6, C-20; 39.9, C-21; 26.3, C-22; 123.9, C-23; 131.5, C-24; 25.7, C-25; 17.7, C-26) by the HMBC correlations from δ_H 1.62 (Me-20) to C-18, C-19, and C-21, from both δ_H 1.67 (Me-25) and 1.59 (Me-26) to C-23 and C-24, coupled with the proton spin systems of H_2-17/δ_H 4.74 (H-18) and δ_H 1.97 (H_2-21)/δ_H 2.03 (H_2-22)/δ_H 5.02 (H-23) in the ^{1}H–^{1}H COSY spectrum. The HMBC correlations of both doublet methyls at δ_H 1.16 and 1.09 with C-7 assigned the location of the isopropyl group (δ_C 39.8, C-8; 18.5, C-9; 18.1, C-10) (Fig. 3).

Besides the aforementioned 26 carbon signals in the ^{13}C and DEPT NMR spectra of **1**, the remaining 15 resonances assignable to three nonprotonated carbons (δ_C 135.5, C-8′; 92.4, C-1′; and 33.8, C-4′), three methines

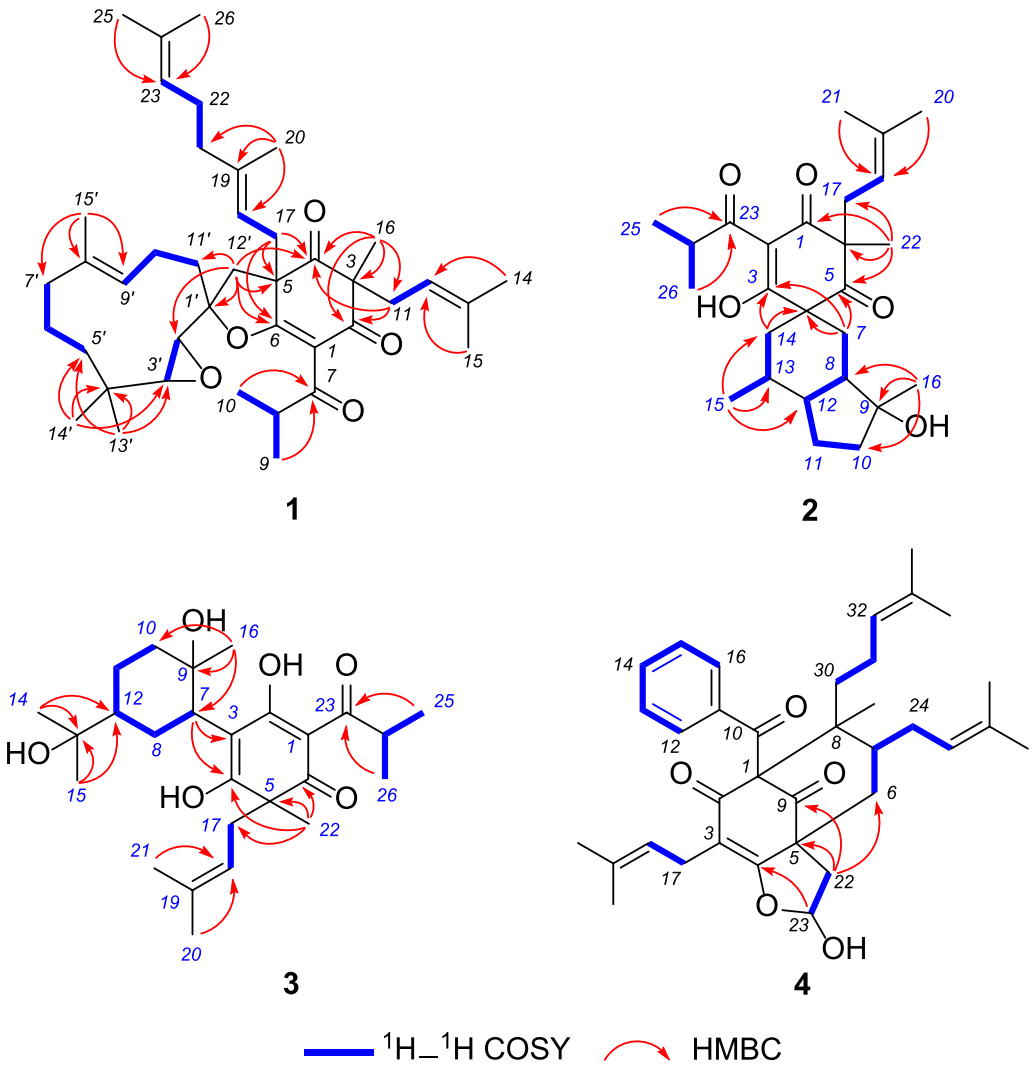

Fig. 3 ^{1}H–^{1}H COSY and HMBC correlations of **1**–**4**

(δ_C 123.6, C-9′; 64.2, C-3′; and 59.4, C-2′), six methylenes, and three methyls indicated a humulane-type sesquiterpenoid moiety. This deduction was further confirmed by the correlations of 2.63 (H-2′)/δ_H 2.85 (H-3′), and δ_H 1.24 (H-5′)/δ_H 1.41 (H-6′)/δ_H 1.76 (H-7′), and δ_H 5.13 (H-9′)/δ_H 2.41 (H-10′)/δ_H 1.71 (H-11′) in the ^{1}H–^{1}H COSY spectrum, along with the HMBC correlations from δ_H 2.31 (H-12′) to δ_C 92.4 (C-1′), 59.4 (C-2′), and 40.3 (C-11′), from both singlet methyls at δ_H 0.64 (Me-14′) and 1.00 (Me-13′) to δ_C 64.2 (C-3′), 33.8 (C-4′), and 39.3 (C-5′), and from singlet methyl at δ_H 1.64 (H-15′) to δ_C 39.5 (C-7′), 135.5 (C-8′), and 123.6 (C-9′) (Fig. 3).

The linkage of C-5/C-12′ was deduced by the HMBC correlations from H_2-12′ to C-4, C-5, and C-6, which combined the acylphloroglucinol and sesquiterpenoid moieties. The formation of the 2′,3′-epoxide and deduced furan ring were indicated by the indices of hydrogen deficiency along with the special chemical shifts of C-1′ (δ_C 92.4), C-2′ (δ_C 59.4), C-3′ (δ_C 64.2), and C-6 (δ_C 178.7). So far, the planar structure of **1** was elucidated as shown (Fig. 1).

Comparison of the structure of **1** with that of hyperkouytin C (**6**) [31] indicated that the benzoyl and prenyl groups in **6** were replaced by an isobutyryl and a methyl in **1**, respectively. The ^{13}C chemical shifts of carbons around C-1′, C-2′ C-3′, and C-5 chiral centers are very close to those of **6**, which suggests that the relative configurations of C-1′, C-2′ C-3′, and C-5 are identical to those of **6**. Furthermore, the chemical shift of H-17a (δ_H 3.29) was 1.01 ppm downfield of H-17b (δ_H 2.28), indicating that compound **1** had a close O2′/H-17a contact

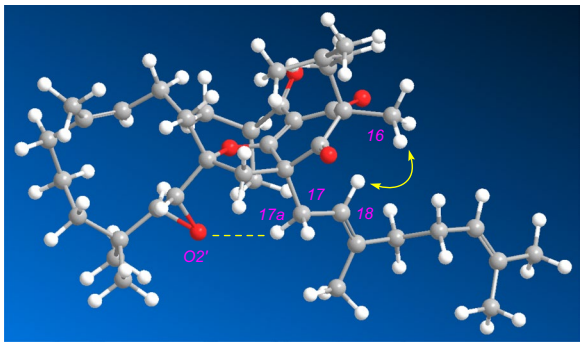

Fig. 4 Configuration optimized molecular model of **1**. yellow arrows, key NOE correlation; yellow dashed line, close O2′/H-17a contact

and the geranyl group was located at the same side of C-2′. This deduction was confirmed by a computationally optimized model (Fig. 4) and the crystallographic data of hypulatone B and hyperkouytins A and B [14, 31]. These evidences further confirmed the relative configurations four chiral carbons mentioned above. Finally, the NOESY correlation between Me-16 and H-18 established the configuration of C-3, thus assigning the relative configuration of **1** as 3*S**, 5*S**, 1′*R**, 2′*R**, 3′*S** (Fig. 4). Considering that all the meroterpenoids of this type were reported in enantiomeric pairs [14, 31], the optical rotation of **1** ($[\alpha]_D = +19$) suggested it might be scalemic mixtures. Nevertheless, the lack of sufficient sample quantities precluded the further chiral separation.

Hypulatone D (**2**) was assigned the molecular formula $C_{26}H_{38}O_5$ by analysis of its ^{13}C NMR (Table 2) and HREIMS data (*m/z* 429.2643 $[M-H]^-$). Comparing the ^1H and ^{13}C NMR data of **2** to those of hyperpatulone E [15] indicates that they are structurally similar. The *sec*-butyl group in hyperpatulone E is replaced by an isopropyl (δ_H 1.21, d; 1.13, d; 3.51, sept.; $J = 6.8$ Hz) in **2**, as evidenced by the HMBC correlations from Me-25 (δ_H 1.21) and Me-26 (δ_H 1.13) to δ_C 206.7 (C-23). It is worth noting that one could barely determine the relative configuration of spirocyclic PPAPs characterized by six chiral centers, like **2**, unless one used a combination of ^1H–^1H coupling constants, conformational analysis, and NOE correlations. Firstly, in the ^1H spectrum of **2** measured in $CDCl_3$ (Table S1), the ^3J coupling constant of H-14b (δ_H 1.23, t, $J = 13.0$ Hz) was 13.0 Hz. So, the corresponding six-membered ring adopted chair conformations (Fig. 5), and H-14a (δ_H 2.00, brd, $J = 13.0$ Hz) and Me-15 were equatorial while H-14b and H-13 (δ_H 1.25) were axial. Secondly, the NOE contacts of Me-15 with H-11_{eq} (δ_H 1.86) and of H-11_{ax} (δ_H 1.11) with H-8 (δ_H 1.57) indicated the trans configuration of the octahydro-indene moiety, as well as the relationship between H-12 and H-13. Thirdly, due to the constraints of the spirocyclic framework, the phloroglucinol ring is perpendicular to the octahydro-indene moiety, which itself lies nearly coplanar with the plane formed by the two C-6 substituents. The NOE correlations of H-14a/Me-22 (δ_H 1.43), H-18 (δ_H 4.70)/H-7b (δ_H 1.79), and H-7b/Me-16 (δ_H 1.28) measured in CD_3OD defined the relative configurations of C-6 and C-9. Thus, the structure of **2** was determined as shown and named as hypulatone D (Fig. 1).

The molecular formula of hypulatone E (**3**) was determined as $C_{26}H_{40}O_6$ by analysis of its ^{13}C NMR (Table 2) and HRESIMS data (*m/z* 447.2745 $[M-H]^-$). The ^1H and ^{13}C NMR data of **3** resembled those of hyperhenone E (**15**) [32]. Instead of two olefinic carbons in hyperhenone E, an oxygen-bearing quaternary carbon at δ_C 73.2 (C-13) and a methyl at δ_C 27.2 (Me-14) appeared in **3**, suggesting that **3** could be derived from hyperhenone E by adding water across the $\Delta^{13,14}$ double bond of the latter. This suggestion was further supported by the correlations of both Me-14 (δ_H 1.15) and Me-15 (δ_H 1.14) with C-13 and C-12 (δ_C 50.8). The NOE contacts of H-7 (3.18) with H-12 (1.48) and Me-16 (1.16) indicated that the relative configurations of C-7, C-9, and C-12 were identical to those of hyperhenone E. Furthermore, the well matched ECD curves of **3** and hyperhenone E (**15**) suggested that their absolute configuration of C-5 was identical [32–34]. Considering that compounds **3** and **15** were co-isolated and the absolute configuration of **15** was determined by X-ray diffraction data [33], the absolute configuration of **3** could be defined as 5*R*, 7*R*, 9*R*, 12*S* (Fig. 1).

The molecular formula of hypulatone F (**4**) was determined to be $C_{35}H_{44}O_5$ from its HRESIMS and ^{13}C NMR data (Table 2). On the basis of analysis of its 1D and 2D NMR data, compound **4** was assigned to possess the same backbone as hypseudohenrin F [35]. The structural novelty of **4** involved the presence of a hemiacetal hydroxyl (δ_H 3.62, OH-23) rather than a methoxy group, which was confirmed by the ^1H–^1H COSY correlations of H-22a (δ_H 2.59) with H-23 (δ_H 6.05), in combination with the HMBC correlations from H-22a to C-5 (δ_C 58.4) and C-6 (δ_C 40.2) and C-9 (δ_C 204.7), and from H-23 to C-4 (δ_C 171.8) (Fig. 3). The 2D NMR data showed that the other structural features of **4** were identical to those of hypseudohenrin F.

Twenty-four known compounds were identified as hypulatone A (**5**) [14], (+)-hyperkouytin C (**6**) [31], hypulatone B (**7**) [14], (−)-hyperkouytin D (**8**) [31], tomoeone A (**9**) [36], tomoeone B (**10**) [36], chipericumin D (**11**) [37], chipericumin E (**12**) [38], hypercohone G (**13**) [39], spirohypatone A (**14**) [13], hyperhenone E (**15**) [32], bellumone I (**16**) [40], hyphenrone J (**17**) [23], hyphenrone K (**18**) [23], hyphenol J (**19**) [34], uralione E (**20**) [41], hookerione K (**21**) [42], attenuatumione D (**22**) [43], sampsonione H (**23**) [44], hypersampsone D (**24**)

Table 2 ^{13}C (150 MHz) and ^{1}H NMR (600 MHz) data of compounds **2**–**4**

No	2 (CD_3OD)		3 (CD_3OD)		4 ($CDCl_3$)	
	δ_C, type	δ_H mult. (*J* in Hz)	δ_C, type	δ_H mult. (*J* in Hz)	δ_C, type	δ_H mult. (*J* in Hz)
1	198.5, C		105.6, C		79.7, C	
2	112.9, C		191.1, C		193.6, C	
3	198.8, C		111.3, C		116.7, C	
4	66.4, C		179.3, C		171.8, C	
5	210.0, C		54.8, C		58.4, C	
6	57.5, C		198.9, C		40.2, CH_2	2.90, dd (14.0, 6.0)
						1.93, d (14.0)
7	27.1, CH_2	1.86, t (13.0)	42.8, CH	3.18, dd (12.4, 3.2)	43.9, CH	1.84, overlap
		1.79, m				
8	51.3, CH	1.54, m	41.1, CH_2	1.83, m	49.1, C	
				1.55, m		
9	79.8, C		73.2, C		204.7, C	
10	41.2, CH_2	1.79, overlap	28.0, CH_2	1.78, t (12.5)	194.0, C	
		1.71, m		1.43, m		
11	27.9, CH_2	1.84, m	23.5, CH_2	1.67, m	137.0, C	
		1.09, m		1.61, m		
12	49.9, CH	1.23, overlap	50.8, CH	1.48, m	128.1, CH	7.43, d (7.7)
13	36.4, CH	1.22, overlap	73.2, C		127.9, CH	7.22, t (7.8)
14	45.0, CH_2	2.06, brd (10.1)	27.2, CH_3	1.15, s	132.0, CH	7.38, t (7.7)
		1.21, overlap				
15	20.3, CH_3	0.87, d (5.0)	26.8, CH_3	1.14, s	127.9, CH	7.22, t (7.8)
16	26.7, CH_3	1.28, s	28.0, CH_3	1.16, s	128.1, CH	7.43, d (7.7)
17	40.3, CH_2	2.64, dd (13.3, 8.2)	40.1, CH_2	2.63, dd (14.0, 7.3)	22.4, CH_2	3.11, m
		2.45, dd (13.3, 8.2)		2.58, dd (14.0, 6.4)		3.04, dd (14.1, 7.2)
18	118.9, CH	4.70, t (8.2)	120.5, CH	4.84, overlap	120.2, CH	5.09, overlap
19	138.1, C		135.4, C		132.9, C	
20	26.1, CH_3	1.55, s	26.2, CH_3	1.54, s	25.8, CH_3	1.62, s
21	17.9, CH_3	1.45, s	18.1, CH_3	1.58, s	17.7, CH_3	1.65, s
22	23.0, CH_3	1.43, s	24.8, CH_3	1.32, s	36.4, CH_2	2.59, m
						1.71, overlap
23	206.7, C		208.5, C		102.4, CH	6.05, d (5.6)
					OH	3.62, brs
24	35.6, CH	3.51, sept (6.8)	36.8, CH	3.98, sept (6.8)	25.5, CH_2	2.28, m
						1.99, m
25	20.1, CH_3	1.21, d (6.8)	19.5, CH_3	1.11, d (6.8)	124.7, CH	5.09, overlap
26	19.3, CH_3	1.13, d (6.8)	19.3, CH_3	1.10, d (6.8)	131.1, C	
27					25.8, CH_3	1.63, s
28					18.0 CH_3	1.65, s
29					13.7, CH3	1.19, s
30					36.4, CH_2	2.21, overlap
						1.41, td (14.0, 5.0)
31					27.1, CH_2	2.23, overlap
						1.84, overlap
32					122.2, CH	5.02, t (7.1)
33					133.4, C	
34					25.5, CH_3	1.59, s
35					17.8, CH_3	1.71, s

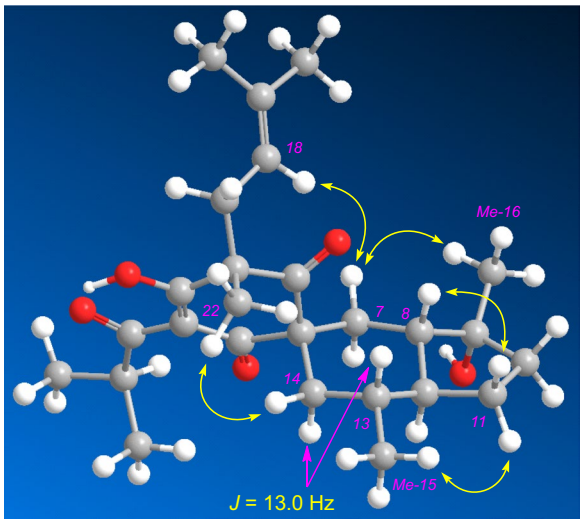

Fig. 5 Configuration optimized molecular model of **2**. Pink arrows, coupling constants; yellow arrows, NOE correlations

Table 3 Cytotoxicity of compounds **1**–**28** on two cancer cell lines with IC_{50} values (μM)

Compound	Huh-7	Panc-1	Compound	Huh-7	Panc-1
1	35.9 ± 3.3	48.4 ± 6.9	**16**	42.1 ± 2.8	45.4 ± 4.9
2	40.2 ± 1.1	> 50	**17**	23.0 ± 2.6	18.6 ± 1.2
3	> 50	41.4 ± 2.1	**18**	34.6 ± 0.4	23.4 ± 1.3
4	32.3 ± 3.7	35.5 ± 1.6	**19**	24.9 ± 2.5	> 50
5	17.3 ± 0.7	20.7 ± 1.8	**20**	17.5 ± 0.5	22.8 ± 2.7
6	19.2 ± 1.0	12.6 ± 0.8	**21**	36.8 ± 3.6	37.3 ± 2.5
7	21.8 ± 1.0	17.4 ± 0.4	**22**	10.0 ± 0.4	> 50
8	10.4 ± 0.2	15.5 ± 0.8	**23**	> 50	> 50
9	36.7 ± 0.7	> 50	**24**	> 50	> 50
10	43.0 ± 3.0	> 50	**25**	41.9 ± 2.3	48.5 ± 3.4
11	29.6 ± 0.9	> 50	**26**	27.3 ± 0.6	21.7 ± 1.6
12	> 50	> 50	**27**	30.8 ± 0.7	42.0 ± 3.8
13	27.2 ± 0.8	> 50	**28**	44.0 ± 2.5	16.3 ± 1.0
14	20.3 ± 0.5	20.4 ± 0.6	Sorafenib	7.4 ± 0.4	8.3 ± 1.3
15	9.7 ± 1.0	11.5 ± 0.5	Paclitaxel	8.1 ± 0.7	3.2 ± 1.3

[45], sampsonione D (**25**) [44], sampsonione C (**26**) [44], hypersampsone I (**27**) [46], and hypersampsonone G (**28**) [47], by comparison of their spectroscopic and physical data with those of related literature (Fig. 2).

All the isolates (compounds **1**–**28**) were tested for their cytotoxic activities on Huh-7 and Panc-1 cell lines by CCK-8 assay. Sorafenib and paclitaxel were used as the positive control. As shown in Table 3, compounds **6**, **8**, and **15** showed moderate inhibitory activity against two human cancer cell lines with IC_{50} values in the range of 9.7–19.2 μM.

In summary, four previously undescribed PAPs, hypulatones C–F (**1**–**4**), together with twenty-four known analogues, were isolated from the fruit of *Hypericum patulum* and structurally characterized. Compounds **6**, **8**, and **15** showed moderate inhibitory activity against two human cancer cell lines with IC_{50} values in the range of 9.7–19.2 μM. Our findings enriched the structural diversity of natural PAPs, and also provided a useful method for configurational assignments of spirocyclic PPAPs that bear six chiral centers.

3 Experimental procedures

3.1 General experimental procedures

Optical rotations were measured on a Jasco P-1020 polarimeter. UV spectra were recorded on a Shimadzu UV-2401PC spectrometer. IR spectra were recorded on a Bruker FT-IR Tensor-27 infrared spectrophotometer with KBr disks. 1D and 2D NMR spectra were recorded on a Bruker DRX-600 spectrometer using TMS as an internal standard. Unless otherwise specified, chemical shifts (δ) are expressed in ppm with reference to the solvent signals. ESIMS and HREIMS data were acquired on Waters Xevo TQS and Waters AutoSpec Premier P776 mass spectrometers, respectively. Semi-preparative HPLC was performed on an Agilent 1100 HPLC with a Zorbarx SB-C_{18} (9.4 × 250 mm) column. Silica gel (200–300 mesh, Qingdao Marine Chemical Co., Ltd., Qingdao, People's Republic of China) were used for column chromatography. Fractions were monitored by TLC (GF 254, Qingdao Marine Chemical Co., Ltd.), and spots were visualized by heating silica gel plates immersed in H_2SO_4 in EtOH.

3.2 Plant materials

The fruits of *Hypericum patulum* were collected in Xishan of Kunming County, Yunan Province, People's Republic of China, in July 2020. The plant was identified by Dr. L. Zhang, and a voucher specimen (KIB 20200701) has been deposited at the Kunming Institute of Botany.

3.3 Extraction and isolation

The dried fruits of *Hypericum patulum* (3.12 kg) were powdered and percolated with MeOH (3 × 10 L) at room temperature for 24 h to yield an extract (680 g) after evaporation in vacuo. The residue was suspended in H_2O and partitioned with EtOAc and H_2O to yield the EtOAc fraction (350 g). This fraction was subjected to column chromatography over silica gel eluted with a petroleum ether–EtOAc in gradient (19:1, 9:1, 8:2, 7:3, 1:1, and 0:1) to obtain 10 fractions (Fr. A–J).

Fr. A (18.6 g) was fractionated by MCI gel column chromatography (MeOH–H_2O, 70:30–100:0) to provide five subfractions (Fr. A1–A5). Fr. A3 (3.1 g) was

fractionated by silica column chromatography using petroleum ether–EtOAc (100:1–0:1) as eluents to provide four subfractions (Fr. A3.1–A3.4). Fr. A3.2 (715 mg) was then purified by semipreparative HPLC (MeOH–H_2O, 92:8) to produce compounds **23** (9.1 mg) and **27** (30.8 mg). Fr. A4 (1.9 g) was then fractionated by silica gel column chromatography using petroleum ether–EtOAc (50:1–0:1) as eluents to provide four subfractions (Fr. A4.1–A4.4). Fr. A4.2 (540 mg) was then purified by semipreparative HPLC eluting with MeOH–H_2O (95:5), in combination with preparative TLC, to afford compounds **1** (2.6 mg), **7** (4 mg), **21** (7 mg), **24** (9.9 mg) and **25** (6 mg). Fr. A4.3 (175 mg) was then fractionated by semipreparative HPLC (MeOH–H_2O, 94:6) to produce compounds **5** (8 mg), **6** (1.3 mg), and **8** (15.7 mg). A portion of Fr. B (6.8 g) was fractionated by MCI gel column chromatography (MeOH–H_2O, 60:40–100:0) to provide five subfractions (Fr. B1–B5). Fr. B5 (3.5 g) was chromatographed on a silica gel column, eluting with petroleum ether–EtOAc (20:1–0:1), to gather Fr. B5.1–B5.3. Compounds **16** (3.9 mg), **17** (6 mg), and **18** (4.1 mg) were obtained from Fr. B5.2 by semipreparative HPLC (MeOH–H_2O, 95:5). Using semipreparative HPLC (MeCN–H_2O, 85:15 and 70:30, respectively), Fr. B4 (639 mg) afforded compounds **10** (4.8 mg) and **15** (89.4 mg). Fr. C (38.5 g) was fractionated by using MCI gel column chromatography (MeOH–H_2O, 40:60–100:0) to gather Fr. C1–C5. Fr. C5 was chromatographed on a silica gel column (petroleum ether–EtOAc, 20:1–0:1) to provide five subfractions (Fr. C5.1–C5.5). Using semipreparative HPLC (MeCN–H_2O, 85:15) and preparative TLC (petroleum ether–EtOAc), compounds **11** (33 mg), **20** (5 mg), **28** (28.1 mg) from Fr. C5.4 (889.5 mg), and compounds **4** (12.3 mg), **9** (3.2 mg), **22** (18.3 mg), and **26** (28.3 mg) from Fr. C5.5 (48.9 mg) were isolated. Similarly, compounds **2** (3.1 mg), **3** (4.5 mg), **12** (13.2 mg), **13** (3.1 mg), **14** (6.3 mg), and **19** (3.9 mg) were obtained from Fr. E (60 g) by using silica gel column, semipreparative HPLC (MeCN – H_2O, 70:30), and preparative TLC.

*Hypulatone C (**1**):* Yellow gum; $[\alpha]_D^{25}$ +19 (*c* 0.1, MeOH); UV (MeOH) λ_{max} (log ε) 210 (4.28), 230 (4.31), 275 (4.28) nm; IR (KBr) ν_{max} 2964, 2930, 2872, 2857, 1719, 1699, 1625, 1456, 1383, 1250, 1184, 1095, 1030, 908, 803 cm^{-1}; ^1H and ^{13}C NMR data, see Table 1. ESIMS *m/z* 671 $[M+K]^+$; HRESIMS *m/z* 671.4082 (calcd for $C_{41}H_{60}O_5K$, 671.4072).

*Hypulatone D (**2**):* Yellow gum; $[\alpha]_D^{25}$ −12 (*c* 0.1, MeOH); UV (MeOH) λ_{max} (log ε) 240 (2.89), 283 (3.02) nm; CD (*c* 3×10^{-4}, MeOH) λ_{max} nm ($\Delta\varepsilon$) 201 (−5.23), 221 (+10.95), 244 (+9.96), 272 (+9.50), 295 (−1.82), 305 (+1.13), 334 (−2.83); IR (KBr) ν_{max} 3317, 2945, 2831, 1668, 1533, 1448, 1279, 1022 cm^{-1}; ^1H and ^{13}C NMR data, see Table 2. ESIMS *m/z* 429 $[M-H]^-$; HRESIMS *m/z* 429.2643 (calcd for $C_{26}H_{37}O_5$, 429.2641).

*Hypulatone E (**3**):* Light yellow gum; $[\alpha]_D^{25}$ +112 (*c* 0.1, MeOH); UV (MeOH) λ_{max} (log ε) 228 (3.07), 238 (3.02), 279 (2.90), 327 (2.97) nm; CD (*c* 3×10^{-4}, MeOH) λ_{max} nm ($\Delta\varepsilon$) 199 (−18.6), 228 (+4.52), 248 (+0.29), 270 (+7.74), 317 (+10.39), 350 (+5.35); IR (KBr) ν_{max} 3334, 3084, 1637, 1502, 1022 cm^{-1}; ^1H and ^{13}C NMR data, see Table 2. ESIMS *m/z* 447 $[M-H]^-$; HRESIMS *m/z* 447.2745 (calcd for $C_{26}H_{39}O_6$, 447.2747).

*Hypulatone F (**4**):* Light yellow gum; $[\alpha]_D^{25}$ −23 (*c* 0.1, MeOH); UV (MeOH) λ_{max} (log ε) 210 (4.25), 248 (4.30), 275 (4.18) nm; IR (KBr) ν_{max} 3437, 2967, 2925, 2859, 1728, 1695, 1627, 1448, 1340, 1317, 1227, 1190,1142, 1057,869, 799, 768, 689 cm^{-1}; ^1H and ^{13}C NMR data, see Table 2. HRESIMS *m/z* 583.2826 (calcd for $C_{35}H_{44}O_5K$, 583.2820).

3.4 Cytotoxicity assay

Cells (Huh-7 and Panc-1) were seeded in 96-well plates at a density of 1×10^4 cells per well, incubated for 24 h, and treated with the different concentrations of all isolated compounds (3.125, 6.25, 12.5, 25, and 50 μM) at 37 °C in 5% CO_2 for another 24 h. A 10 μL amount of the Cell Counting Kit-8 (Biosharp, Shanghai, China) was added to the medium and incubated for 2 − 4 h; then the absorbance was read at a wavelength of 450 nm using a microplate reader (Shenzhen Sanli Technology Co. Ltd, Shenzhen, China). Sorafenib (G-CLONE, Beijing, China) and paclitaxel (G-CLONE, Beijing, China) were used as positive control [27]. The half-maximal inhibitory concentration (IC_{50}) value was measured and calculated by GraphPad Prism 8 software.

Supplementary Information

The online version contains supplementary material available at https://doi.org/10.1007/s13659-026-00629-9.

Supplementary material 1. ^1H and ^{13}C NMR data for compounds **2** and **3** in $CDCl_3$ (Table S1), Original MS and NMR spectra of compounds **1**–**4** (Figs. S1–S44).

Acknowledgements

The authors would like to thank the Natural Sciences Foundation of Guangdong Province (No. 2025A1515010551) and the Shenzhen Medical Research Funds (A2303041). The project was also funded by Shanghai Pujiang Program (No. 2021PJD091) and Shenzhen High-level Hospital Construction Fund (GSP-ZDSYS-009, GSP-QNPY-A2025004).

Author contributions

Xing-Wei Yang and Juan Huang conceived and designed the study. Yu-Feng Qiu and Yi-Zhou performed the isolation and purification of the compounds. Yu-Feng Qiu and Cheng Chen performed the pharmacological experiments and analysis of the data. The manuscript has been drafted by Yu-Feng Qiu and revised by Xing-Wei Yang. All authors have read and agreed to the published version.

Data availability
All data generated or analyzed during this study are included in this published article and its supplementary information files.

Declarations

Competing interests
The authors declare no competing financial interest.

Author details
[1]School of Pharmaceutical Sciences (Shenzhen), Sun Yat-Sen University, Shenzhen 518107, People's Republic of China. [2]State Key Laboratory of Cardiovascular Disease, Fuwai Shenzhen Hospital, Chinese Academy of Medical Sciences, Shenzhen 518057, China. [3]Department of Pharmacology, Shanghai Medicilon Inc., Shanghai, China.

Received: 6 January 2026 Accepted: 12 March 2026
Published online: 23 April 2026

References

1. Yang XW, Grossman RB, Xu G. Research progress of polycyclic polyprenylated acylphloroglucinols. Chem Rev. 2018;118(7):3508–58.
2. Ciochina R, Grossman RB. Polycyclic polyprenylated acylphloroglucinols. Chem Rev. 2006;106(9):3963–86.
3. Li XW, Li J, Stevens P. Flora of China. Beijing: Science Press; 1990. p. 25.
4. State Administration of Traditional Chinese Medicine of the People's Republic of China, Chinese Materia Medica, Shanghai Scientific and Technical Publishers, Shanghai. 1999;9:594–608.
5. Ishiguro K, Nagareya N, Suitani A, Fukumoto H. A prenylated xanthone from cell suspension cultures of *Hypericum patulum*. Phytochemistry. 1997;44(6):1065–6.
6. Tanaka N, Yano Y, Tatano Y, Kashiwada Y. Hypatulins A and B, meroterpenes from *Hypericum patulum*. Org Lett. 2016;18:5360–3.
7. Liu YY, Ao Z, Xue GM, Wang XB, Luo JG, Kong LY. Hypatulone A, a homoadamantane-type acylphloroglucinol with an intricately caged core from *Hypericum patulum*. Org Lett. 2018;20:7953–6.
8. Liu YY, Ao Z, Xu QQ, Zhu DR, Chen C, Wang XB, et al. Hyperpatulols A–I, spirocyclic acylphloroglucinol derivatives with anti-migration activities from the flowers of *Hypericum patulum*. Bioorg Chem. 2019;87:409–16.
9. Wu ZN, Niu QW, Zhang YB, Luo D, Li QG, Li YY, et al. Hyperpatulones A–F, polycyclic polyprenylated acylphloroglucinols from *Hypericum patulum* and their cytotoxic activities. RSC Adv. 2019;9:7961–6.
10. Tanaka N, Niwal K, Yano Y, Kashiwada Y. Prenylated benzophenone derivatives from *Hypericum patulum*. J Nat Med. 2020;74:264–8.
11. Ao Z, Liu YY, Lin YL, Chen XL, Chen K, Kong LY, et al. Hyperpatulones A and B, two new peroxide polyprenylated acylphloroglucinols from the leaves of *Hypericum patulum*. Tetrahedron Lett. 2020;61:151385.
12. Jia XY, Wu YM, Lei C, Yu YY, Li JQ, Li JY, et al. Hyperinoids A and B, two polycyclic meroterpenoids from *Hypericum patulum*. Chin Chem Lett. 2020;31:1263–6.
13. Ye YS, Jiang NN, Yang XW, Xu G. Polycyclic polyprenylated acylphloroglucinol with an unprecedented spirocyclic core from *Hypericum patulum*. Chin Chem Lett. 2020;31:2433–6.
14. Ye YS, Du SZ, Jiang NN, Xu HX, Yang J, Fu WW, et al. Novel meroterpenoids from *Hypericum patulum*: highly potent late $Na_v1.5$ sodium current inhibitors. Org Lett. 2020;22:6339–43.
15. Zhang YX, Ao Z, He YW, Lu JY, Chen XL, Kong LY, et al. Hyperpatulones C-G, new spirocyclic polycyclic polyprenylated acylphloroglucinols from the leaves of *Hypericum patulum*. Fitoterapia. 2021;155:105063.
16. Duan YL, Deng YF, Bu PF, Xie SS, Guo Y, Shi ZY, et al. Discovery of nor-bicyclic polyprenylated acylphloroglucinols possessing diverse architectures with anti-hepatoma activities from *Hypericum patulum*. Bioorg Chem. 2021;111:104902.
17. Zhang F, Yang J, Yi P, Li YN, Hao XJ, Yuan CM. Hyperpatone A, a polycyclic polyprenylated acylphloroglucinol with a rare 8/6/5/6/5 pentacyclic skeleton from *Hypericum patulum*. Org Biomol Chem. 2023;21:140–6.
18. Yang XW, Deng X, Liu X, Wu CY, Li XN, Wu B, et al. Hypercohin A, a new polycyclic polyprenylated acylphloroglucinol possessing an unusual bicyclo[5.3.1]hendecane core from *Hypericum cohaerens*. Chem Commun. 2012;48(48):5998–6000.
19. Luo Y, Grossman RB, Nie XB, Yang XW. Total synthesis and structural reassignment of garcinielliptone FC, a polycyclic polyprenylated acylphloroglucinol with diverse bioactivity. Chem Commun. 2023;59(41):6215–8.
20. Yang XW, Ding Y, Zhang JJ, Liu X, Yang LX, Li XN, et al. New acylphloroglucinol derivatives with diverse architectures from *Hypericum henryi*. Org Lett. 2014;16(9):2434–7.
21. Hu YL, Hu K, Kong LM, Xia F, Yang XW, Xu G. Norascyrononones A and B, 2,3,4- nor-polycyclic polyprenylated acylphloroglucinols from *Hypericum ascyron*. Org Lett. 2019;21(4):1007–10.
22. Yang XW, Grossman RB. Revision of the structure of hypatulone A by NMR, computations, and biosynthetic considerations. Org Lett. 2020;22(2):760–3.
23. Yang XW, Li MM, Liu X, Ferreira D, Ding Y, Zhang JJ, et al. Polycyclic polyprenylated acylphloroglucinol congeners possessing diverse structures from *Hypericum henryi*. J Nat Prod. 2015;78(4):885–95.
24. Yang XW, Yang J, Xu G. Skeleton reassignment of type C polycyclic polyprenylated acylphloroglucinols. J Nat Prod. 2017;80(1):108–13.
25. Grossman RB, Yang XW. Structural revision of garcinielliptin oxide and garcinielliptone E. J Nat Prod. 2020;83(6):2041–4.
26. Wang X, Nie XB, Grossman RB, Ji TF, Yang XW. Structural revision of hyperibrin B and hyperscabrones H and I by biosynthetic considerations, NMR analysis, and chemical synthesis. J Nat Prod. 2021;84(7):2059–64.
27. Xu ZH, Grossman RB, Qiu YF, Luo Y, Lan T, Yang XW. Polycyclic polyprenylated acylphloroglucinols bearing a lavandulyl-derived substituent from *Garcinia xanthochymus* fruits. J Nat Prod. 2022;85(12):2845–55.
28. Qiu YF, Grossman RB, Yang XW. Structure revision of type B polycyclic polyprenylated acylphloroglucinols fused to a partly reduced furan ring. J Nat Prod. 2023;86(10):2391–7.
29. Xu ZH, Luo Y, Qiu YF, Yang XW, Lan T. Prenylated acylphloroglucinols from the fruits of *Garcinia xanthochymus*. Fitoterapia. 2023;165:105427.
30. Fu Y, Huang YQ, Xu Z, Liu X, Yang XW. Polyprenylated acylphloroglucinols from *Garcinia* species and structural revision of seven analogues. Nat Prod Bioprospect. 2025;15:34.
31. Huang JC, Sheng L, Zong JF, Zhou YB, Li J, Hou AJ. Enantiomeric pairs of meroterpenoids with 11/5/6 spiro-heterocyclic systems from *Hypericum kouytchense*. Org Chem Front. 2022;9(23):6475–83.
32. Zhang JJ, Yang XW, Ma JZ, Ye Y, Shen XL, Xu G. Cytotoxic polyprenylated acylphloroglucinol derivatives from *Hypericum henryi*. Tetrahedron. 2015;71:8315–9.
33. Ye YS, Wu M, Jiang NN, Lao YZ, Fu WW, Liu X, et al. Dearomatized isoprenylated acylphloroglucinol derivatives with potential antitumor activities from *Hypericum henryi*. Nat Prod Bioprospect. 2020;10:1–11.
34. Jiang NN, Yue GGL, Li P, Ye YS, Gomes AJ, Kwok FHF, et al. Discovery of dearomatized isoprenylated acylphloroglucinols with colon tumor suppressive activities in mice via inhibiting NFκB-FAT1-PDCD4 signaling activation. Eur J Med Chem. 2022;239:114532.
35. Sun H, Wang J, Zhen B, Wang X, Suo X, Lin M, et al. Polycyclic polyprenylated acylphloroglucinol derivatives from *Hypericum pseudohenryi*. Phytochemistry. 2021;187:112761.
36. Hashida W, Tanaka N, Kashiwada Y, Sekiya M, Ikeshiro Y, Takaishi Y. Tomoeones A–H, cytotoxic phloroglucinol derivatives from *Hypericum ascyron*. Phytochemistry. 2008;69:2225–30.
37. Abe S, Tanaka N, Kobayashi J. Prenylated acylphloroglucinols, chipericumins A-D, from *Hypericum chinense*. J Nat Prod. 2012;75(3):484–8.
38. Tala MF, Talontsi FM, Zeng GZ, Wabo HK, Tan NH, Spiteller M, et al. Antimicrobial and cytotoxic constituents from native Cameroonian medicinal plant *Hypericum riparium*. Fitoterapia. 2015;102:149–55.
39. Zhang JJ, Yang XW, Ma JZ, Liu X, Yang LX, Yang SC, et al. Hypercohones D–G, new polycyclic polyprenylated acylphloroglucinol type natural products from *Hypericum cohaerens*. Nat Prod Bioprospect. 2014;4:73–9.
40. Zhou X, Xu WJ, Li YR, Zhang MH, Tang PF, Lu WJ, et al. Anti-inflammatory, antioxidant, and anti-nonalcoholic steatohepatitis acylphloroglucinol meroterpenoids from *Hypericum bellum* flowers. J Agric Food Chem. 2021;69:646–54.
41. Zhou ZB, Li ZR, Wang XB, Luo JG, Kong LY. Polycyclic polyprenylated derivatives from *Hypericum uralum*: neuroprotective effects and antidepressant-like activity of uralodin A. J Nat Prod. 2016;79:1231–40.

42. Ye Y, Yang XW, Zhou Y, Xu G. Homo-adamantane type polycyclic polyprenylated acylphloroglucinols from *Hypericum hookerianum*. Fitoterapia. 2019;133:43–50.
43. Zhou ZB, Zhang YM, Pan K, Luo JG, Kong LY. Cytotoxic polycyclic polyprenylated acylphloroglucinols from *Hypericum attenuatum*. Fitoterapia. 2014;95:1–7.
44. Hu LH, Sim KY. Sampsoniones C–H, a unique family of polyprenylated benzophenone derivatives with the novel tetracyclo[7.3.1.1^{3,11}.0^{3,7}] tetradecane-2,12,14-trione skeleton, from *Hypericum sampsonii* (Guttiferae). Tetrahedron Lett. 1999;40:759–62.
45. Lin YL, Wu YS. Polyprenylated phloroglucinol derivatives from *Hypericum sampsonii*. Helv Chim Acta. 2003;86:2156–63.
46. Zeng YH, Osman K, Xiao ZY, Gibbons S, Mu Q. Four geranyl-bearing polyisoprenylated benzoylphloroglucinol derivatives from *Hypericum sampsonii*. Phytochem Lett. 2012;5:200–5.
47. Zhang JS, Zou YH, Guo YQ, Li ZZ, Tang GH, Yin S. Polycyclic polyprenylated acylphloroglucinols: natural phosphodiesterase-4 inhibitors from *Hypericum sampsonii*. RSC Adv. 2016;6:53469–76.

Publisher's Note